

Polyconjugated Polymers from Anodic Coupling of Dipyrrolyl–Ethylenes, –Arylenes, and –Heteroarylenes. Narrow Potential Windows of Conductivity by Alternation of Electron-Rich and Electron-Poor Units

Gianni Zotti,* Sandro Zecchin, and Gilberto Schiavon

Istituto di Polarografia ed Elettrochimica Preparativa, Consiglio Nazionale delle Ricerche, c.o Stati Uniti 4, 35020 Padova, Italy

Anna Berlin,* Giorgio Pagani, and Michela Borgonovo

Dipartimento di Chimica Organica e Industriale dell'Università e Centro CNR Speciali Sistemi Organici, via C. Golgi 19, 20133 Milano, Italy

R. Lazzaroni

Service de Chemie des Materiaux Nouveaux, Centre de Recherche en Electronique and Photonique Moleculaires, Universite' de Mons-Hainaut, Place du Parc 20, B-7000 Mons, Belgium

Received April 10, 1997. Revised Manuscript Received July 7, 1997[Ⓢ]

Anodic coupling of a series of dipyrrolyl–ethylenes, –thiophenes, –phenylenes, and –diethylene–thiophenes has produced new conducting polyconjugated polymers ($\sigma = 3 \times 10^{-3}$ to 15 S cm^{-1}). The polymers have been characterized by cyclic voltammetry, UV–vis spectroscopy, electrochemical quartz crystal microbalance, in situ ESR and in situ conductivity. Alternation of electron-rich (dipyrrole) and electron-poor (ethylene and/or arylene) moieties in the polyconjugated chain produces the appearance of one (or two in some cases) narrow potential windows of conductivity during the oxidative doping process. The relationship between the width of the cyclic voltammogram, the presence of conductivity windows, and the polymer structure is discussed.

Introduction

Alternation of electron-acceptor (A) and -donor (D) moieties in a polyconjugated polymer has been the object of several investigations^{1–9} that are performed with two main purposes. The first is the obtainment of low-bandgap polymers. Alternating D and A units strong enough to make the respective HOMO and LUMO levels close would yield a low-gap material.² In fact the use of weak donor and acceptors such as thiophene (D) and pyridine (A) units was not satisfactory,¹ whereas the polymers containing squarate or croconate (A) and benzopyrrolines or benzothiazoles (D) units² and those constituted by benzothiadiazole (A) and thiophene or *N*-methylpyrrole (D) units⁵ were successful.

A second target is the preparation of molecular quantum wells, possibly useful for the production of highly efficient organic LEDs thanks to the introduction of well-defined luminescence centers.¹⁰ A–D polymers investigated in this context are for instance polythiophenes containing alternating alkoxy- and bromo-³ or cyano-substituted⁴ thiophene units.

Alternation of D and A units in a polyconjugated polymer may give rise to charge localization with effects also in the conductive behavior. To explore this aspect, we devised polymer films from anodic coupling of monomers constituted by regularly alternating D and A conjugated units, which in practice means trimers with D–A–D or A–D–A sequences. The former possibility was selected in order to localize the unpaired electron of the reacting radical cation at the terminal unit and therefore to ease the coupling process. Finally, to increase the A–D alternation to a reasonably high level, the selected D unit was pyrrole while the A spacers were variously substituted ethylene, arylene, or heteroarylene units. Following these ideas we have considered monomers **1–8**, shown in Figure 1. The project was extended to longer conjugated sequences such as those displayed by **9** and **10**. The latter

* Correspondence should be addressed to gzotti@pdadr1.pd.cnr.it

Ⓢ Abstract published in *Advance ACS Abstracts*, October 1, 1997.

(1) Zhou, Z.; Maruyama, T.; Kanbara, T.; Ikeda, T.; Uchimura, K.; Yamamoto, T.; Tokuda, K. *J. Chem. Soc., Chem. Commun.* **1991**, 1210.

(2) Havinga, E. E.; Hoeve, W. T.; Wynberg, H. *Polym. Bull.* **1992**, 29, 119.

(3) Faid, K.; Leclerc, M.; Nguyen, M.; Diaz, A. *Macromolecules* **1995**, 28, 284.

(4) Demanze, F.; Yassar, A.; Garnier, F. *Adv. Mater.* **1995**, 7, 907.

(5) Kitamura, C.; Tanaka, S.; Yamashita, Y. *Chem. Mater.* **1996**, 8, 570.

(6) Effenberger, F.; Wurthner, F.; Steybe, F. *J. Org. Chem.* **1995**, 60, 2082.

(7) Yamamoto, T.; Zhou, Z.; Kanbara, T.; Shimura, M.; Kizu, K.; Maruyama, T.; Nakamura, Y.; Fukuda, T.; Lee, B.L.; Ooba, N.; Tomaru, S.; Kurihara, T.; Kaino, T.; Kubota, K.; Sasaki, S. *J. Am. Chem. Soc.* **1996**, 118, 10389.

(8) Ho, H. A.; Brisset, H.; Elandaloussi, E. H.; Frere, P.; Roncali, J. *Adv. Mater.* **1996**, 8, 990.

(9) Gasmi, A.B.; Frere, P.; Roncali, J. *J. Electroanal. Chem.* **1996**, 406, 231.

(10) Ruckh, R.; Sigmund, E.; Kollmar, C.; Sixl, H. *J. Chem. Phys.* **1986**, 85, 2797.

(11) Berlin, A.; Wernet, W.; Wegner, G. *Makromol. Chem.* **1987**, 188, 2963.

(12) Reynolds, J. R.; Katritzky, A. R.; Soloduchko, J.; Belyakov, S.; Sotzing, G. A.; Pyo, M. *Macromolecules* **1994**, 27, 7225.

(13) Sotzing, G. A.; Reynolds, J. R.; Katritzky, A. R.; Soloduchko, J.; Belyakov, S.; Musgrove, R. *Macromolecules* **1996**, 29, 1679.

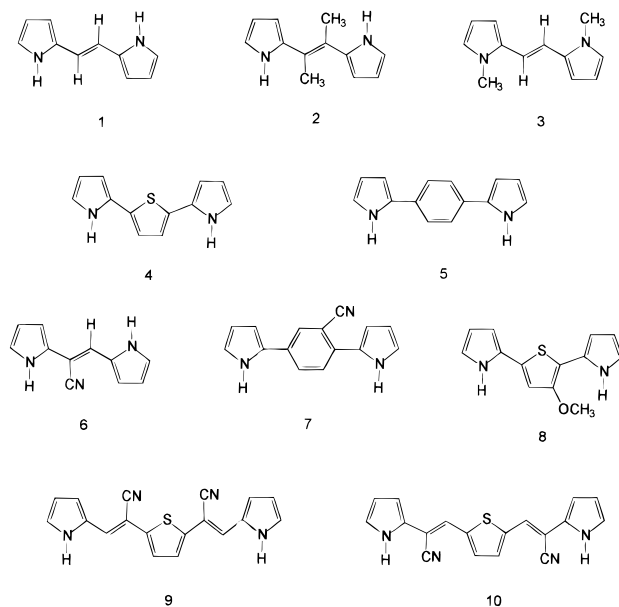


Figure 1. Structures of dipyrrolyl-ethylenes, -arylenes and -heteroarylenes.

symmetrical isomers differ for the position of the cyano groups with respect to the central thiophene and external pyrrole rings. The synthesis and polymerization of **3**¹¹ and **5**^{12,13} were previously reported. Also recently reported are the analogous *N*-methyl-substituted **4** and **5**.¹⁴

This paper reports the synthesis and oxidative polymerization of these compounds in acetonitrile, the characterization of the resulting polymer films, and the evolution of their conductivity during oxidative doping.

Experimental Section

Chemicals and Reagents. All melting points are uncorrected. All reactions of air- and water-sensitive materials were performed under nitrogen. Air- and water-sensitive solutions were transferred with double-ended needles. The solvents used in the reactions were dried by conventional methods and freshly distilled under nitrogen. Acetonitrile (AN) was reagent grade (Uvasol, Merck) with a water content <0.01%. The supporting electrolyte tetrabutylammonium perchlorate (Bu₄NClO₄) was previously dried under vacuum at 70 °C. All other chemicals were reagent grade and used as received.

The following compounds were prepared according to literature prescriptions: 1,4-bis(pyrrol-2-yl)-1,4-butanedione,¹⁵ *N*-[(trimethylsilyl)ethoxymethyl]pyrrole (*N*-Sem-pyrrole),¹⁶ 2,5-dibromo-3-methoxythiophene,¹⁷ 2,5-dibromobenzonitrile,¹⁸ 2,5-bis(cyanomethyl)thiophene,¹⁹ pyrrol-2-ylacetonitrile,²⁰ thiophene-2,5-dicarbaldehyde,²¹ nickel(II) [1,3-bis(diphenylphosphino)propane] chloride (NiCl₂(dppp)).²²

The synthesis of compounds **1–3** and **6** was previously reported.²³

¹H NMR spectra were recorded on a Bruker AC 300 (300 MHz for ¹H); chemical shift values are given in ppm and are referred to tetramethylsilane. Electron-impact mass spectra (EI-MS) were taken on a VG 7070 EQ-HF spectrometer.

2,5-Bis(pyrrol-2-yl)thiophene (4). A mixture of 1,4-bis(pyrrol-2-yl)-1,4-butanedione (300 mg, 1.39 mmol) and Lawesson's reagent (444 mg, 1.09 mmol) in dry toluene (18 mL) was refluxed for 2 h. The reaction mixture was cooled to room temperature, poured into water, and extracted with ether. The organic phase was dried (Na₂SO₄), and the solvent evaporated. Flash chromatography (silica gel, petrol ether/ether 6:4) of the residue afforded **4** (152 mg, 65% yield) as a pale green solid, mp 195 °C dec (lit.²⁴ mp 194–196 °C). Anal. Calcd for C₁₂H₁₀N₂S: C, 67.29; H, 4.67; N, 13.07%. Found: C, 67.12; H, 4.60; N, 12.95%. ¹H NMR (CDCl₃) δ 6.25 (2 H, m, β pyrrole protons), 6.38 (2 H, m, β pyrrole protons), 6.80 (2 H, m, α pyrrole protons), 6.90 (2 H, s, thiophene protons), 8.30 (2 H, broad s, NH).

1,4-Bis(*N*-Sem-pyrrol-2-yl)benzene. *t*-BuLi (1.5 M in hexane, 2.36 mL, 3.55 mmol) was added dropwise to a solution of *N*-Sem-pyrrole (700 mg, 3.55 mmol) in hexane (5 mL) keeping the temperature at –10 °C. After 30 min the yellow solution was stirred for a further 30 min at room temperature. After cooling to –30 °C, a solution of ZnCl₂ (484 mg, 3.55 mmol) in THF (6 mL) was added dropwise, and the reaction mixture stirred for 2 h at 0 °C. NiCl₂(dppp) (18 mg) was added, and after the temperature was lowered again to –30 °C, a solution of 1,4-dibromobenzene (411 mg, 1.74 mmol) in THF (6 mL) was added dropwise. After reaching room temperature, the reaction mixture was heated at 50 °C for 3 h, cooled to room temperature, poured into water saturated with NaHCO₃, and extracted with ether. The organic phase was washed with water and dried (Na₂SO₄), and the solvent evaporated. Flash chromatography (silica gel, petrol ether/ether 9:1) of the residue afforded 1,4-bis(*N*-Sem-pyrrol-2-yl)benzene (293 mg, 36% yield) as a green solid, mp 134 °C. Anal. Calcd for C₂₆H₄₀N₂O₂Si₂: C, 66.66; H, 8.54; N, 5.98%. Found: C, 66.51; H, 8.63; N, 5.75%. ¹H NMR (CDCl₃) δ 0.03 (18 H, s, CH₃), 0.89 (4 H, t, CH₂Si), 3.45 (4 H, t, OCH₂), 5.20 (4 H, s, NCH₂), 6.25 (2 H, m, β pyrrole protons), 6.35 (2 H, m, β pyrrole protons), 6.85 (2 H, m, α pyrrole protons), 7.52 (4 H, s, benzene protons).

1,4-Bis(pyrrol-2-yl)benzene (5). A mixture of 1,4-bis(*N*-Sem-pyrrol-2-yl)benzene (150 mg, 0.32 mmol), ethylenediamine (0.5 mL), Bu₄NF supported on silica gel (1.25 mmol of F[–]/g of silica gel, 4.28 g, 3.21 mmol), and DMF (10 mL) was heated at 50 °C for 80 h. After cooling to room temperature, the reaction mixture was filtered, and the solid washed several times with CH₂Cl₂. The combined organic fractions were washed with water and dried (Na₂SO₄). Removal of the solvent at reduced pressure and flash chromatography (silica gel, petrol ether/ether 4:6) of the residue afforded **5** (37 mg, 55% yield) as a pale green solid, mp decomposes between 295 and 300 °C (lit.²⁹ mp decomposes between 298 and 307 °C, lit.¹³ mp 170 °C). Anal. Calcd for C₁₄H₁₂N₂: C, 80.78; H, 5.76; N, 13.45%. Found: C, 80.59; H, 5.70; N, 13.32%. ¹H NMR (CDCl₃) δ 6.28 (2 H, m, β pyrrole protons), 6.58 (2 H, m, β pyrrole protons), 6.87 (2 H, m, α pyrrole protons), 7.25 (4 H, s, benzene protons), 8.42 (2 H, broad s, NH).

1,4-Bis(*N*-Sem-pyrrol-2-yl)-2-cyanobenzene. This compound was prepared following the same procedure described for 1,4-bis(*N*-Sem-pyrrol-2-yl)benzene, using in this case 2,5-dibromobenzonitrile (450 mg, 1.72 mmol). Flash chromatography (silica gel, petrol ether/ether 9:1) of the residue afforded the title compound (314 mg, 37% yield) as a green oil. Anal. Calcd for C₂₇H₃₉N₃O₂Si₂: C, 65.72; H, 7.90; N, 8.51%. Found: C, 65.56; H, 7.75; N, 8.36%. ¹H NMR (CDCl₃) δ 0.06 (9 H, s,

(14) Geissler, U.; Hallensleben, M. L.; Rhode, N. *Macromol. Chem. Phys.* **1996**, *197*, 2565.

(15) Chierici, L.; Serventi, G. *Gazz. Chim. Ital.* **1956**, *55*, 2904.

(16) Muchowski, J.; Solas, R. *J. Org. Chem.* **1984**, *49*, 203.

(17) Rossi, R.; Carpita, A.; Ciofalo, M.; Lippolis, V. *Tetrahedron* **1991**, *47*, 8843.

(18) Pearson, D. E.; Pope, H. W.; Hargrove, W. *Org. Synth.* **1960**, *40*, 7.

(19) Badger, G. M.; Elix, J. A.; Lewis, G. E. *Aust. J. Chem.* **1965**, *18*, 70.

(20) Hertz, W.; Dittmer, K.; Crestal, S. J. *J. Am. Chem. Soc.* **1947**, *68*, 1968.

(21) Stretter, H.; Rajh, B. *Chem. Ber.* **1976**, *109*, 534.

(22) Kumada, M.; Tamao, K.; Sumitani, K. *Org. Synth.* **1978**, *58*, 127.

(23) Pagani, G.; Berlin, A.; Canavesi, A.; Schiavon, G.; Zecchin, S.; Zotti, G. *Adv. Mater.* **1996**, *8*, 819.

(24) Merrill, B. A.; LeGoff, E. *J. Org. Chem.* **1990**, *55*, 2904.

(25) Lucchesini, F. *Tetrahedron* **1992**, *48*, 9951.

(26) Zotti, G.; Schiavon, G. *Synth. Met.* **1989**, *31*, 347.

(27) Diaz, A. *Chem. Scr.* **1981**, *17*, 145.

(28) Zotti, G.; Schiavon, G.; Berlin, A.; Pagani, G. *Synth. Met.* **1993**, *60*, 179.

(29) Schiavon, G.; Sitran, S.; Zotti, G. *Synth. Met.* **1989**, *32*, 209.

CH_3), 0.09 (9 H, s, CH_3), 0.87 (2 H, t, CH_2Si), 0.91 (2 H, t, CH_2Si), 3.15 (2 H, t, OCH_2), 3.30 (2 H, t, OCH_2), 5.18 (2 H, s, NCH_2), 5.20 (2 H, s, NCH_2), 6.25 (1 H, m, β pyrrole proton), 6.32 (1 H, m, β pyrrole proton), 6.38 (1 H, m, β pyrrole proton), 6.58 (1 H, m, β pyrrole proton), 6.89 (1 H, m, α pyrrole proton), 6.96 (1 H, m, α pyrrole proton), 7.67 (1 H, d, $J = 8.2$ Hz, benzene H^6), 7.81 (1 H, dd, $J = 8.2$ and 1.7 Hz, benzene H^5), 7.98 (1 H, d, $J = 1.7$ Hz, benzene H^3).

1,4-Bis(pyrrol-2-yl)-2-cyanobenzene (7). The same procedure as for the obtainment of **5** was used starting from 1,4-bis(*N*-Sem-pyrrol-2-yl)-2-cyanobenzene (290 mg, 0.58 mmol). Flash chromatography (silica gel, petrol ether/ether 3:7) of the residue afforded **7** (112 mg, 82% yield) as a yellow solid, mp 203 °C. Anal. Calcd for $C_{15}H_{11}N_3$: C, 77.26; H, 4.72; N, 18.01%. Found: C, 77.12; H, 4.56; N, 17.87%. 1H NMR (DMSO- d_6) δ 6.15 (1 H, m, β pyrrole proton), 6.21 (1 H, m, β pyrrole proton), 6.70 (1 H, m, β pyrrole proton), 6.83 (1 H, β pyrrole proton), 6.91 (1 H, α pyrrole proton), 7.00 (1 H, m, α pyrrole proton), 7.70 (1 H, d, $J = 8.5$ Hz, benzene H^6), 7.91 (1 H, dd, $J = 8.5$ and 1.9 Hz, benzene H^5), 8.05 (1 H, d, $J = 1.9$ Hz, benzene H^3) 11.45 (2 H, broad d, *NH*). MS, *m/e* 233 (M^+).

2,5-Bis(*N*-Sem-pyrrol-2-yl)-3-methoxythiophene. *t*-Bu-Li (1.5 M in hexane, 4.05 mL, 6.08 mmol) was added dropwise to a solution of *N*-Sem-pyrrole (1.20 g, 6.09 mmol) in hexane (10 mL), keeping the temperature at -10 °C. The reaction mixture was allowed to reach room temperature and stirred for 30 min. After cooling to -65 °C, a solution of Me_3SnCl (1.25 g, 6.27 mmol) in THF (10 mL) was added dropwise, and the reaction mixture stirred for 4 h at the same temperature and for a further 24 h at room temperature. $(PPh_3)_2PdCl_2$ (220 mg) was added, and after the temperature was lowered to -30 °C, a solution of 2,5-dibromo-3-methoxythiophene (540 mg, 1.99 mmol) in THF (9 mL) was added dropwise. After coming up to room temperature, the reaction mixture was refluxed for 4 h. The temperature was lowered again to -30 °C and a solution of *N*-Sem-2-(trimethylstannyl)pyrrole, prepared as described above from *N*-Sem-pyrrole (1.20 g, 6.09 mmol) and Me_3SnCl (1.25 g, 6.27 mmol), was added dropwise. After warming to room temperature, the reaction mixture was then refluxed for 4 h, cooled to room temperature, poured into water, and extracted with ether. The organic phase was dried (Na_2SO_4), and the solvent evaporated. Flash chromatography (silica gel, petrol ether/ether 9:1) of the residue afforded 2,5-bis(*N*-Sem-pyrrol-2-yl)-3-methoxythiophene (351 mg, 35% yield) as a green oil. Anal. Calcd for $C_{25}H_{40}N_2O_3SSi_2$: C, 59.52; H, 7.93; N, 5.55%. Found: C, 59.37; H, 7.85; N, 5.39%. 1H NMR ($CDCl_3$) δ 0.06 (9 H, s, $Si(CH_3)_3$), 0.09 (9 H, s, $Si(CH_3)_3$), 0.89 (2 H, t, CH_2Si), 0.91 (2 H, t, CH_2Si), 3.34 (2 H, t, OCH_2), 3.54 (2 H, t, OCH_2), 3.80 (3 H, s, OCH_3), 5.26 (2 H, s, NCH_2), 5.28 (2 H, s, NCH_2), 6.18 (1 H, m, β pyrrole proton), 6.24 (1 H, m, β pyrrole proton), 6.27 (1 H, m, β pyrrole proton), 6.38 (1 H, m, β pyrrole proton), 6.85 (1 H, m, α pyrrole proton), 6.89 (1 H, m, α pyrrole proton), 7.09 (1 H, s, thiophene proton).

2,5-Bis(pyrrol-2-yl)-3-methoxythiophene (8). The same procedure as for the production of **5** was used, starting from 2,5-bis(*N*-Sem-pyrrol-2-yl)-3-methoxythiophene (270 mg, 0.53 mmol). Flash chromatography (silica gel, petrol ether/ether 4:6) of the residue afforded **8** (65 mg, 50% yield) as a green solid, mp 135 °C. Anal. Calcd for $C_{13}H_{12}N_2OS$: C, 63.94; H, 4.91; N, 11.47%. Found: C, 63.70; H, 4.82; N, 11.36%. 1H NMR ($CDCl_3$) δ 3.98 (3 H, s, OCH_3), 6.21 (1 H, m, β pyrrole proton), 6.25 (1 H, m, β pyrrole proton), 6.39 (1 H, m, β pyrrole proton), 6.77–6.83 (3 H, m, α pyrrole and thiophene protons), 8.22 (1 H, broad s, *NH*), 9.32 (1 H, broad s, *NH*). MS, *m/e* 244 (M^+).

2,5-Bis[1-cyano-2-(pyrrol-2-yl)vinyl]thiophene (9). Triton B (40% in methanol, 0.5 mL) was added to a refluxing ethanol solution (1.5 mL) of a mixture of 2-pyrrolaldehyde (120 mg, 1.23 mmol) and 2,5-bis(cyanomethyl)thiophene (100 mg, 0.61 mmol). Heating was continued for 15 min, and then the solvent evaporated. Water was added, and the solid filtered with suction. The product was purified by sublimation (180 °C, 0.5 mmHg) to give **9** (97 mg, 50% yield) as a red solid, mp 214 °C. Anal. Calcd for $C_{18}H_{12}N_4S$: C, 68.37; H, 3.79; N, 17.70%. Found: C, 68.45; H, 3.70; N, 17.56%. 1H NMR ($CDCl_3$) δ 6.35 (2 H, m, β pyrrole protons), 6.69 (2 H, m, β

pyrrole protons), 7.08 (2 H, m, α pyrrole protons), 7.12 (2 H, s, $CN=CH$ or thiophene protons), 7.14 (2 H, s, $CN=CH$ or thiophene protons), 9.51 (2 H, broad s, *NH*). MS, *m/e* 316 (M^+).

2,5-Bis[2-cyano-2-(pyrrol-2-yl)vinyl]thiophene (10). Triton B (40% in methanol, 2.3 mL) was added to a refluxing ethanol solution (14 mL) of a mixture of thiophene-2,5-dicarbaldehyde (1.00 g, 7.14 mmol) and pyrrol-2-ylacetonitrile (1.50 g, 14.10 mmol). Heating was continued for 15 min, and then the solvent evaporated. Water was added, and the solid filtered with suction. Flash chromatography (silica gel, CH_2Cl_2) of the product afforded **10** (587 mg, 26% yield) as a dark red solid, mp 235–240 °C (dec). Anal. Calcd for $C_{18}H_{12}N_4S$: C, 68.37; H, 3.79; N, 17.70%. Found: C, 68.23; H, 3.69; N, 17.65%. 1H NMR (DMSO- d_6) δ 6.21 (2 H, m, β pyrrole protons), 6.44 (2 H, m, β pyrrole protons), 7.03 (2 H, α pyrrole protons), 7.58 (2 H, s, $CN=CH$ or thiophene protons), 7.79 (2 H, s, $CN=CH$ or thiophene protons), 11.63 (2 H, broad s, *NH*). MS, *m/e* 316 (M^+).

Electrochemical Apparatus and Procedure. Experiments were performed at 25 °C under nitrogen in three-electrode cells. The counter electrode was platinum; the reference electrode was a silver/0.1 M silver perchlorate in AN (0.34 V vs SCE). The voltammetric apparatus (AMEL, Italy) included a 551 potentiostat modulated by a 568 programmable function generator and coupled to a 731 digital integrator.

The working electrode for cyclic voltammetry was a platinum minidisk electrode (0.003 cm²). For electronic spectroscopy a 0.8 × 2.5 cm indium–tin oxide (ITO) sheet (ca 80% transmittance, ca. 20 Ω sq⁻¹ resistance, from Balzers, Liechtenstein) was used.

ESR spectra were taken on a Bruker ER 100D following the procedure previously described;²⁶ electronic spectra were taken with a Perkin-Elmer Lambda 15 spectrometer.

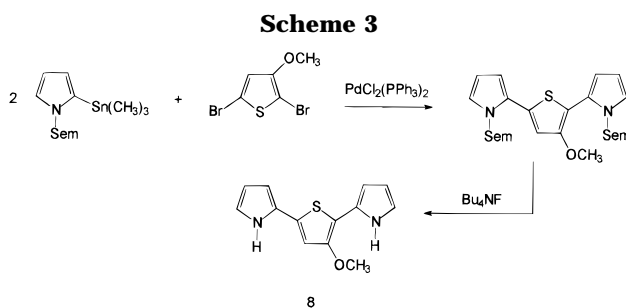
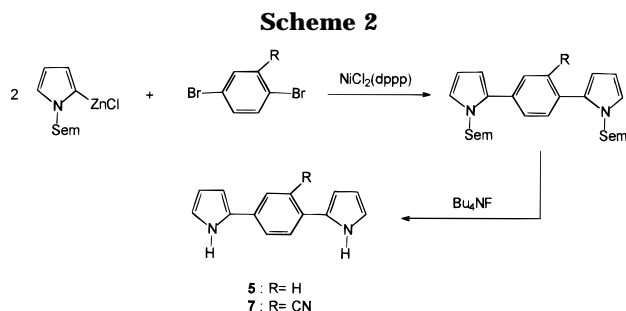
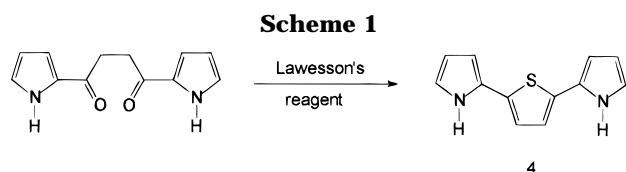
Anodic coupling of the monomers to polymer was performed in $(2-5) \times 10^{-3}$ M monomer solutions in AN + 0.1 M Bu_4NClO_4 with addition of 1% H_2O which improves the polymerization process of pyrroles.²⁷ Poly(1,2-dithienylethylene) films were prepared as reported previously.²⁸

The apparatus and procedures used in the in situ conductivity experiments were previously described in detail.²⁹ The relevant working electrode was a two-band platinum electrode (0.3 cm × 0.01 cm for each band) with interband spacing of 6 μ m, typically polymer-coated with the passage of 20 mC, which ensured the attainment of limiting resistance conditions. Poly(3-methylthiophene) (60 S cm⁻¹) was used as conductivity standard.

EQCM Apparatus and Procedure. Electrochemical quartz crystal microbalance (EQCM) analysis was performed with a gold-coated AT-cut quartz electrode (0.35 cm²), resonating at 6 MHz, onto which the polymers were deposited. The oscillator circuit was homemade, and the frequency counter was Hewlett-Packard Model 5316B. Calibration of the quartz crystal microbalance was performed with silver deposition from a 10^{-2} M solution of $AgNO_3$ in AN + 0.1 M Bu_4NClO_4 .

Measurements were performed outside the depositing solution in order both to measure the mass of polymer films in the dry state and to avoid errors due to polymer roughness.³⁰ The reactivity toward air of the neutral polymers imposed the condition of measuring the mass in the oxidized state and, as a consequence, to take into account the potential dependence of the oxidation level of the polymer. The procedure was therefore that of depositing the polymer potentiostatically (CV cycling was avoided since it introduces extra electrolyte in the films³⁰) and measuring the deposition charge Q_d , then leaving the polymer at open circuit until attainment of equilibrium (steady open-circuit potential), extracting, washing with AN and drying in nitrogen stream to constant mass *m*. Subsequently the film was immersed in the monomer-free solution, its potential checked (it was reproducibly unchanged from the previous equilibrium value), and its charge content Q_{ox} measured by reduction to the neutral state.

(30) Schiavon, G.; Zotti, G.; Comisso, N.; Berlin, A.; Pagani, G. *J. Phys. Chem.* **1994**, *98*, 4861.



Simple correlation of deposition charge Q_d , measured mass m , and charge stored in the as-deposited polymer Q_{ox} , through eqs 1–3:

$$(Q_d - Q_{ox})/nF = m_0/W_m \quad (1)$$

$$(Q_{ox})/F = m_x/W_x \quad (2)$$

$$m = m_0 + m_x \quad (3)$$

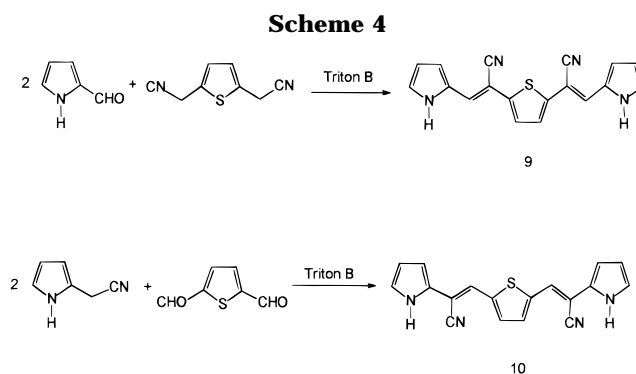
where m_0 and m_x are the masses of the neutral polymer and of the dopant anion, W_m and W_x the molar masses of the monomer and of the anion, allows the determination of the electron stoichiometry of coupling n and the mass of the neutral polymer m_0 .

Results and Discussion

Synthesis of the Monomers. The required pyrrole-based monomers belong to a series of compounds that are not extensively described in the literature.

The synthesis of compounds **1–3** and **6**, all as trans isomers, was described by us previously.²³

As for compound **4**, the synthesis carried out as described in the literature²⁴ resulted to be of very poor yield. We have developed a simpler synthesis of **4**, as depicted in Scheme 1. This is based on the reaction of 1,4-bis(pyrrol-2-yl)-1,4-butanedione with Lawesson's reagent. Two different pathways for the synthesis of **5** in moderate yields have been recently reported.^{13,25} In this paper we propose an alternative route for the obtainment of **5**, which is also of moderate yield but has the advantage that it can be extended to the synthesis of various substituted compounds, such as **7**. This route, depicted in Scheme 2, is based on a cross-coupling reaction (Negishi coupling) between *N*-Sem-pyrrol-2-yl-zinc chloride and the appropriate dibromo derivative



catalyzed by a Ni catalyst. The Sem protecting group can be easily removed by reaction with Bu_4NF .

The methoxy-functionalized compound **8** was also prepared by a cross-coupling reaction, Stille reaction in this case, between *N*-Sem-2-(trimethylstannyl)pyrrole and 2,5-dibromo-3-methoxythiophene in the presence of a Pd catalyst, followed by nitrogen deprotection (Scheme 3). If Negishi coupling is applied, the main reaction product is, in this case, *N*-Sem-2,2'-dipyrrole, and the desired compound can be isolated in trace amount.

Finally isomeric compounds **9** and **10** were prepared by Triton B catalyzed condensation of the proper aldehyde and the appropriate nitrile derivative, as shown in Scheme 4.

Electrosynthesis and CV Analysis of the Polymers. The cyclic voltammogram (CV) of the monomers in AN + 0.1 M Bu_4NClO_4 + 1% H_2O displays a single oxidation peak; continuous cycling of the potential over the peak leads to the growth of an electroactive polymer film (Figure 2).

The CV responses of the polymer films in AN + 0.1 M Bu_4NClO_4 (some representative polymers are shown in Figure 3) are characterized by features dependent on the substitution pattern of the monomers. The monomers bearing a single substituent (**6–8**) are asymmetrical, which makes nonequivalent the terminal α

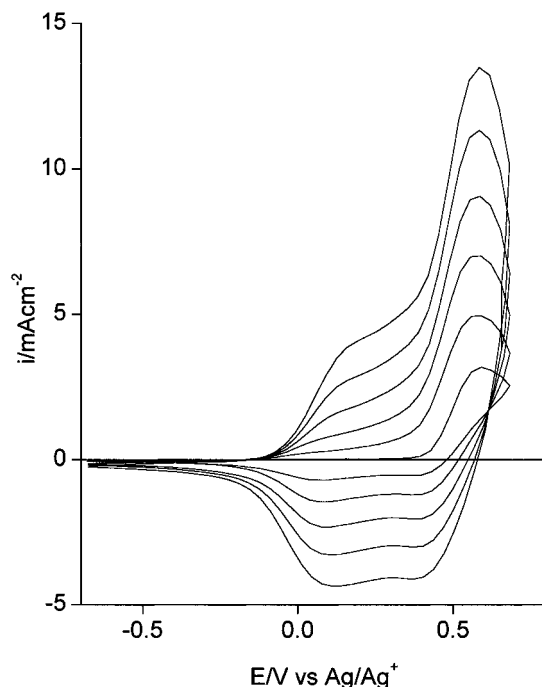


Figure 2. Repetitive cyclic voltammetry for 5×10^{-3} M **9** in AN + 0.1 M Bu_4NClO_4 . Scan rate: 0.1 V s^{-1} .

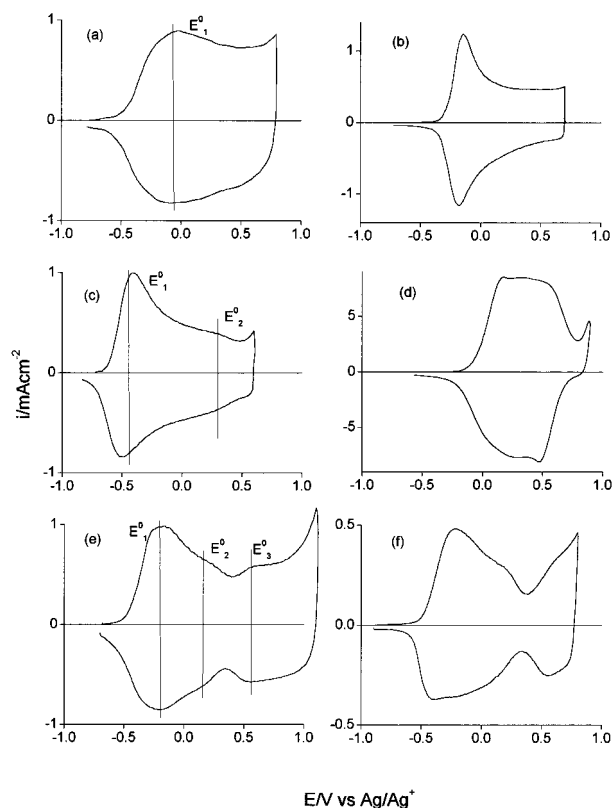


Figure 3. Cyclic voltammetry for (a) poly(**6**) ($Q_r = 6.7 \text{ mC cm}^{-2}$), (b) poly(**3**) ($Q_r = 4.3 \text{ mC cm}^{-2}$), (c) poly(**1**) ($Q_r = 6.7 \text{ mC cm}^{-2}$), (d) poly(**9**) ($Q_r = 50 \text{ mC cm}^{-2}$), (e) poly(**4**) ($Q_r = 10 \text{ mC cm}^{-2}$), and (f) poly(**5**) ($Q_r = 5 \text{ mC cm}^{-2}$) in AN + 0.1 M Bu₄NClO₄. Scan rate: 0.1 V s⁻¹.

positions of the pyrrole ends undergoing the coupling process. Thus while the CV of polymers from the asymmetrical monomers (hereafter designed ASYM) has the usual shape of a rounded peak (at E_1^0) followed by a flat featureless plateau (Figure 3a), the CV pictures of the other polymers (hereafter SYM) show a further rounded peak (at E_2^0) beyond which the current decreases (Figure 3c). For the polymers from **9** and **10**, the twin system is even more evident (Figure 3d). The redox potentials E_1^0 and E_2^0 appear to limit a relatively narrow redox process. A second redox process appears for almost all SYM polymers (starting from $E_3^0 = 0.6\text{--}0.9 \text{ V}$) in which ca. 50% of the charge for the first one is involved, as measured for poly(**4**) and poly(**5**) (e and f in Figure 3) which are the most stable in the oxidized form. The polymer from **3** constitutes a remarkable exception since its CV (Figure 3b) displays a single process despite the symmetry of the monomer.

Given the above features, the reversible charge of SYM polymers was evaluated on the first redox process, while for the ASYM polymers it was measured at a switching potential of 0.6 V, selected for the common stability of the oxidized form toward overoxidation.

The electrochemical parameters of all the polymers (monomer peak potentials and polymer redox potentials) are listed in Table 1. Hereafter we report some characteristics of their electropolymerization, performed by potential cycling, including the charge yield, i.e., the ratio of reversible charge over deposition charge at the neutral state, a parameter useful for the evaluation of the efficiency of the electrodeposition process.

Oxidation of **1**, **4**, **9**, and **10** produces polymers without dissolutive losses, which was evidenced by the

Table 1. Electrochemical and UV-Vis Absorption Data for the Investigated Monomers (Oxidation Peak Potential E_p and Maximum Absorption λ_m) and Polymers (Redox Potential E^0 , Maximum Absorption λ_p , and Optical Gap E_g)

monomer	E_p/V^a	E^0/V^b	λ_m/nm^c	λ_p/nm	E_g/eV
1	0.10	-0.45/0.3/0.7	330	480	2.6
2	0.14	-0.2	286	390	3.2
3	0.12	-0.2	346	400	3.1
4	0.17	-0.3/0.1/0.6	352	470	2.6 ₅
5	0.23	-0.3/0.2/0.65	328	440	2.8
6	0.42	-0.05	377	560	2.2
7	0.45	0.2	328, 370sh	465	2.7
8	0.04	-0.3	365	460	2.7
9	0.56	0.1/0.5/-	442,465sh	540,630sh	2.0
10	0.48	-0.2/0.2/0.85	462,490sh	630,770sh	1.6

^a At a scan rate of 0.1 V s⁻¹ and 10⁻³ M concentration. ^b $E_1^0/E_2^0/E_3^0$. ^c In AN.

absence of coloring of the solution during extensive electrodepositions. From the charge yield at the first redox process (50%) the charge thereby involved corresponds to 1 electron/dipyrrole unit; the charge involved in the second, displayed by **1** and **4**, corresponds to 0.5 electron/dipyrrole unit. Poly(**1**) undergoes oxidative degradation at the second redox process ($E > 0.7 \text{ V}$), whereas poly(**4**) is stable at potentials as high as 1.2 V.

Poly(**9**) and poly(**10**) are also reduced at -1.65 and -1.8 V, respectively, due to the electron-withdrawing properties of the cyano groups and the relatively extended conjugation. The reduction is only partially reversible at low scan rates (typically 0.1 V s⁻¹) being most likely followed by hydrodimerization as previously observed in dithienyl-ethylene polymers.^{31,32}

The polymerization of **5**, already reported in the literature,¹² under our conditions (the same as in the literature plus 1% added water) occurs with a charge yield of ca. 40%, which suggests some losses but points also in this case to the exchange of 1 electron/dipyrrole unit at the first redox process. The second redox process develops at ca. 0.65 V (Figure 3f), but at potentials higher than 0.8 V the polymer suffers of oxidative degradation.

From **3**, **6**, and **7** the polymers are obtained with charge yields of 15, 20, and 30%, respectively. These values indicate significant dissolutive losses, but this was not an obstacle to the production of deposits thick enough for conductivity measurements. Oxidation of **8** gives a polymer with severe losses, which are due in this case to the poor adherence of the material to the electrode. In any case charge yields of 10% may be reached.

Oxidation of **2** produces polymer with a low charge yield (ca. 2%) which is attributed to a high solubility of the oligomers. This property is attributable to the presence of the alkyl substituents forcing the twisting of the pyrrole rings. Due to this difficulty, bridging of the electrode for in situ conductivity measurements was not possible in this case.

EQCM Analysis of the Polymers. To evaluate precisely the electron stoichiometry (i.e., the number of electrons passed per monomer) of the anodic coupling processes (and consequently the degree of polymerization of the resulting polymers) and to determine the

(31) Zotti, G.; Schiavon, G.; Zecchin, S.; Berlin, A.; Pagani, G. *Synth. Met.* **1994**, *66*, 149.

(32) Zotti, G.; Schiavon, G.; Zecchin, S. *Synth. Met.* **1995**, *72*, 275.

Table 2. Conductivity Data (Maximum Conductivity σ_{\max} , Potential of Maximum Conductivity E_{\max} , Conductivity Width at Half-Height CW and Cyclic Voltammetric Width ΔE°) of the Polymers

monomer	$\sigma_{\max}/\text{Scm}^{-1}$	E_{\max}/V	CW/V	$\Delta E^{\circ}/\text{V}^a$
1	15	-0.2	0.70	0.75
3	3×10^{-3} ¹¹			
4	2	-0.05	0.40	0.40
5	0.3	0.1	0.35	0.50
6	2			
7	0.1			
8	0.15			
9	0.5	0.3	0.35	0.40
10	0.5	0.2	0.35	0.40

^a $\Delta E^{\circ} (=E_2^{\circ} - E_1^{\circ})$.

charge involved in the reversible CV processes, we performed an EQCM analysis of the electrodeposition and redox switching of the polymers. The analysis, performed according the procedure outlined in the Experimental Section, was applied to the polymers from **1**, **4**, **9**, and **10**, for which no significant dissolution was observed.

From the calculations (see Experimental Section) the electron stoichiometry of coupling n for **1** and **4** corresponds to 2 electrons/monomer, which indicates that a long-chain polymer is formed. This result is in line with the high degree of polymerization encountered in polypyrroles.³³

For **9** and **10** the charge for coupling corresponds to 1.5 electrons/monomer, which indicates that the polymers are in fact tetramers. On the other hand it is known that coupling of oligomers with extended conjugation produces short polymers.³⁴ In any case when the (potentiostatically produced) deposits undergo potential cycling in monomer-free solution, the tetramers are coupled to polymer with the passage of the required charge, as previously observed for thiophene oligomers.³⁵ Polymers prepared directly by potential cycling do not undergo this extra charge of polymerization, as expected, and are therefore produced with a high degree of polymerization.

Correlation between the mass of the neutral polymer m_0 and the reversible charge Q_r involved in the first redox process has allowed us to state that one electron is exchanged per dipyrrole unit and, since CV analysis has shown that the charge injected at the subsequent process is 50% of the first, 0.5 electron/dipyrrole unit is thereby involved. This result confirms that obtained from the evaluation of the charge yield in CV.

UV-Vis Spectroscopy of the Polymers. The maximum absorptions in the UV-vis spectra of the monomers and of the relevant polymers are reported in Table 1; the energy gaps and band-edge energies for the homopolymers, which are used for the evaluation of the theoretically expected values, are summarized in Table 3 and illustrated in Figure 4.

The maximum absorption of the neutral form of poly(**1**) (2.6 eV) is close to the value of 2.5 eV arising from the weighted average of the energy gaps E_g for polypyrrole and polyacetylene. Thus poly(**1**) obeys a rule that was found to hold in general for polyconjugated

Table 3. Electronic Properties (Valence and Conduction Band Edges as E°_{ox} and E°_{red} and Bandgap E_g) of the Homopolymers

polymer	$E^{\circ}_{\text{ox}}/\text{V}^a$	$E^{\circ}_{\text{red}}/\text{V}^a$	E_g/eV
polypyrrole	-0.25 ⁴⁰	-3.1 ^b	2.85 ⁴⁰
polyacetylene	0.3 ⁴¹	-1.6 ^b	1.9 ⁶⁹
poly(cyanoacetylene)	1.65 ^b	-0.77 ⁰	2.35 ⁷¹
polythiophene	0.45 ⁷²	-1.85 ^b	2.3 ⁷²
poly(<i>N</i> -methylpyrrole)	0.1 ⁷³	-3.9 ^b	4.0 ⁷³
polyparaphenylene	1.4 ⁷⁴	-2.1 ⁷⁴	3.5 ^b

^a Vs SCE reference electrode. ^b Calculated from $E_g = e(E^{\circ}_{\text{ox}} - E^{\circ}_{\text{red}})$.

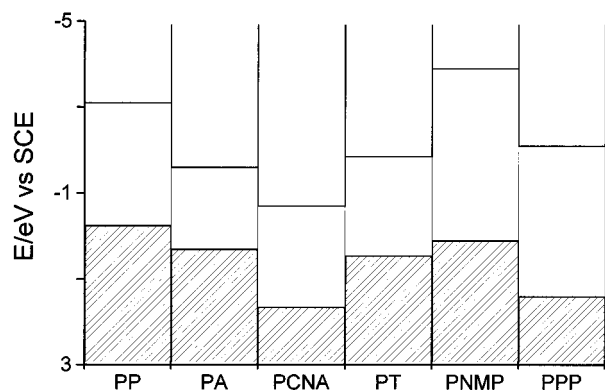


Figure 4. Valence and conduction band edges of the homopolymers. Legend: PP (polypyrrole), PA (polyacetylene), PCNA (polycyanoacetylene), PT (polythiophene), PNMP (poly-*N*-methylpyrrole), PPP (polyparaphenylene).

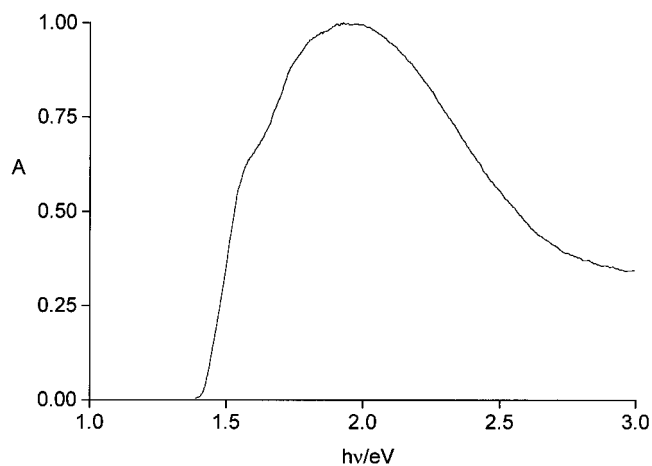


Figure 5. UV-vis spectrum of poly(**10**) on ITO.

copolymers.³⁶ Similarly, for poly(**3**) the gap (3.1 eV) is close to the 3.3 eV value interpolated from those of polyacetylene and poly(*N*-methylpyrrole). For poly(**4**) the interpolated E_g value (2.65 eV) matches exactly the experimental value.

The situation is quite different for poly(**6**), poly(**9**), and poly(**10**). The presence of the cyano groups decreases strongly the energy gaps so that in, e.g., poly(**10**) the spectrum (Figure 5) points to an absorption onset as low as 1.4 eV.

The weight-averaged value of E_g calculated for the cyano-substituted polymers from the corresponding homopolymers is in these cases higher than the experimental energy gap. We suggest that the reason of the marked lowering of E_g must be sought in the conjuga-

(33) Nazzari, A.; Street, G. B. *J. Chem. Soc., Chem. Commun.* **1983**, 83.

(34) Zotti, G.; Gallazzi, M. C.; Zerbi, G.; Meille, S. V. *Synth. Met.* **1995**, *73*, 217.

(35) Zotti, G.; Schiavon, G. *Synth. Met.* **1990**, *39*, 183.

(36) Meyers, F.; Heeger, A. J.; Bredas, J. L. *J. Phys. Chem.* **1992**, *97*, 2750.

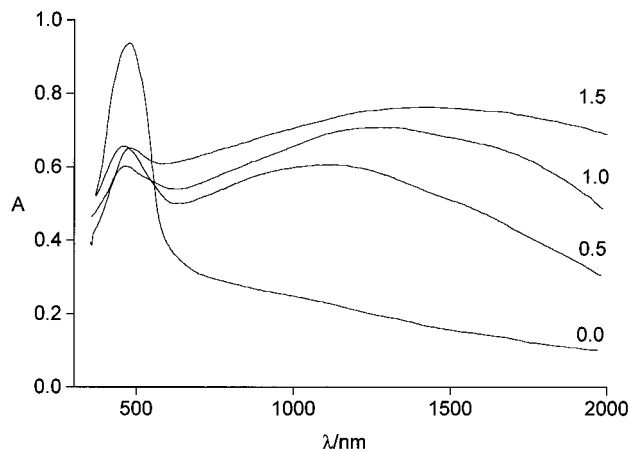


Figure 6. Spectroelectrochemistry of poly(4) in AN + 0.1 M Bu₄NClO₄ at different values of doping level (as electrons per dipyrrole unit).

tion of the cyano group with the ethylene group and thereby with the pyrrole ends, with the consequent stabilization of quinoid structures. If we consider the energy diagram of the homopolymers in Figure 4, we may observe that the conduction band edge for polycyanoacetylene is only 0.45 eV higher than the valence band edge of polypyrrole. This allows a charge-transfer interaction between the cyano and the pyrrole groups and the consequent strong decrease of the energy gap in the polymer.

Comparing poly(9) and poly(10), the gap narrowing appears to be stronger for the former, which is explained by its longer conjugation pathway between the pyrrole and cyano moieties.

A special comment must be devoted to poly(2), which shows the highest value of absorption energy. In fact the spectrum of the monomer itself is strongly blue shifted in comparison with that of 1, a result indicating that steric hindrance twists the molecule, as previously observed in analogous thiophene-based monomers.³⁷ As a consequence the polymer chain has a low degree of conjugation.

Finally, spectroelectrochemistry of poly(4), namely, the polymer which shows two stable redox processes (Figure 3e), has evidenced that oxidation at the second redox process does not introduce new features with respect to the spectrum of the polymer oxidized at the first one (Figure 6).

With progressive oxidation the spectrum shows the appearance first and then the increase of the interband transition of polypyrrole with continuous lowering of the energy gap; at the second redox process the spectrum shows simply a continuation of this evolution.

In Situ Conductivity of the Polymers. In situ conductivity measurements of the polymer deposits shows that oxidation causes the transition from an insulating to a conductive state as generally found in polyconjugated polymers (some significant examples are shown in Figures 7 and 8).

The detailed pattern of conductivity shows in any case novel features and significant differences from polymer to polymer.

Upon oxidation poly(1), a typical SYM polymer, goes from the insulating (neutral) to a low-conductivity state

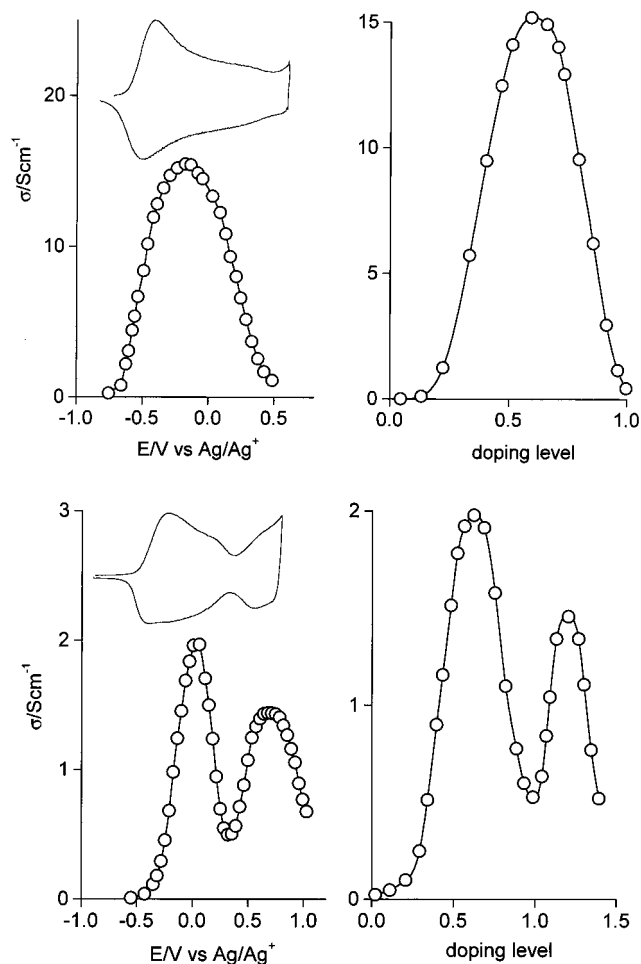


Figure 7. In situ conductivity vs potential and doping level (as electrons per dipyrrole unit) of (a, top) poly(1) and (b, bottom) poly(4) in AN + 0.1 M Bu₄NClO₄. Cyclic voltammograms for comparison.

at the anodic limit of the first redox process through a maximum located roughly midway through the redox process (Figure 7a). A complete valence band depletion of the polymer at the anodic limit is ruled out by the presence of a high CV capacitive current: in fact the polymer remains thereby appreciably conductive. All the other SYM polymers behave similarly. This conductive behavior is completely different from that of polypyrrole (Figure 8a) which is conducting through an extended potential plateau.

The relationship between conductivity and reversible charge is shown for poly(1) in Figure 7a. It can be observed that the conductivity maximum occurs roughly at 50% of the charge stored at the first process, which reminds the maximum conductivity of a half-oxidized redox state.³⁸ A more careful evaluation shows that the maximum is displaced to a significantly higher level of oxidation, 60% of Q_r, with a significant asymmetry of the curve. This result may be accounted for by the dominance of mixed-valence conduction between polaron and bipolaron (rather than neutral and polaron) forms similarly to the behavior of sexithiophene, which is conductive at the mixed cation-dication state.³⁹

To explain the limited potential domain of conductivity, we suggest that the ethylene moiety confines the

(37) Sannicolò, F.; Brenna, E.; Zotti, G.; Schiavon, G.; Zecchin, S., to be published.

(38) Chidsey, C. E. D.; Murray, R. W. *J. Phys. Chem.* **1986**, *90*, 1479.
(39) Zotti, G.; Schiavon, G.; Berlin, A.; Pagani, G. *Adv. Mater.* **1993**, *5*, 551.

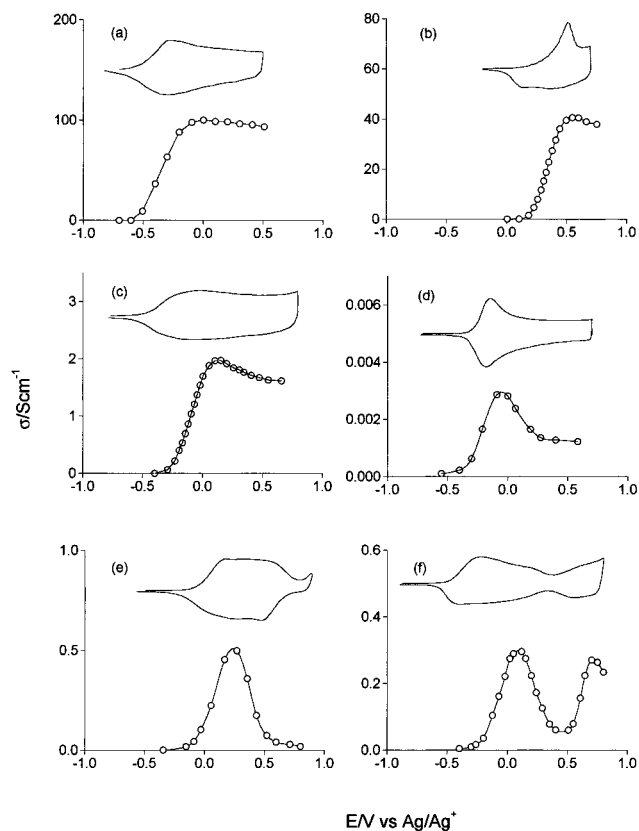


Figure 8. In situ conductivity vs potential for (a) polypyrrole, (b) poly(1,2-dithienylethylene), (c) poly(**6**), (d) poly(**3**), (e) poly(**9**), and (f) poly(**5**) in AN + 0.1 M Bu₄NClO₄. Cyclic voltammograms for comparison.

oxidation charge in the dipyrrole subunits (one positive charge per dipyrrole subunit, first step in Figure 9).

The easier oxidizability of the dipyrrole vs the ethylene unit in poly(**1**) is clearly given by the comparison of the oxidation potentials for polypyrrole (−0.25 V vs SCE⁴⁰) and polyacetylene (0.3 V vs SCE⁴¹). Similar considerations may be used for the other A–D alternating polymers. A regular sequence of discrete dipyrrole units implies a localization of the pyrrole molecular orbitals in bands narrower than in polypyrrole, where this dimerization is obviously absent, with splitting of the valence band of polypyrrole into narrower subbands. The result is the appearance of narrow potential windows of conductivity.

The finding that poly(1,2-dithienylethylene) does not show a maximum of conductivity (Figure 8b) confirms that charge localization is the origin of the narrowing of the potential window of conductivity. In this polymer the thiophene and ethylene moieties are electronically much alike since the sulfur atom does not particularly influence the electronic properties⁴² (Table 3 and Figure 4 show that the valence band edges of the homopolymers are almost at the same level, differing only by 0.15 V, which is statistically lowered to ca. 0.1 V if we consider the double contribution of the thiophene unit). Similarly the decreased donor properties of the dipyrrole unit in poly(**3**), caused by the noncoplanarity of the pyrrole

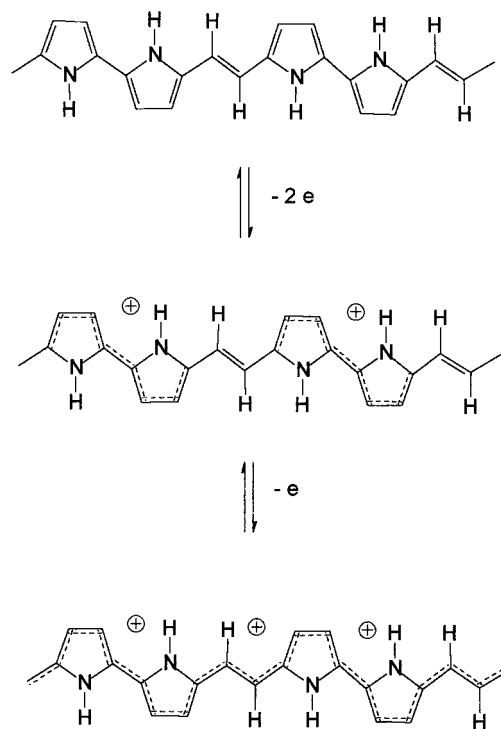


Figure 9. Oxidation processes of poly(**1**).

units, make the dipyrrole and ethylene moieties close in energy (ca. 0.2 V difference, increased to ca. 0.25 V by the double contribution of the pyrrole unit), producing only a limited drop of conductivity (ca. 50%) in the conductivity–potential relationship (Figure 8d). As a side comment, it should be remarked that the conductivity of poly(**3**), which is in agreement with that reported in the literature,¹¹ is low because of the steric hindrance of the *N*-methyl groups.

The conductive behavior of poly(**4**) is even more surprising than for poly(**1**). In this SYM polymer, in which both redox processes are stable, the conductivity shows two windows in their correspondence (Figure 7b). A similar behavior is displayed by poly(**5**) (Figure 8f), even though at the anodic limit of the second redox process the conductivity starts to be affected by degradation with prolonged oxidation. In both cases, the second maximum of conductivity is comparable with the first, which may be explained by substantially unchanged polymer structures and intersite distances. A second window of conductivity, which involves half the charge used for the first, may be explained by a second localization of the additionally injected positive charge, this time on polymer segments constituted by four-pyrrole units formed from dimerization of the dipyrrole units oxidized at the first redox process (second step in Figure 9).

Both poly(**9**) and poly(**10**), the remaining SYM polymers, display the window of conductivity in a particularly clear-cut way, with a maximum centered at the CV process (Figure 8e) and a strong drop of conductivity (ca. 50 times). From the data in Table 2 it is observed that the maximum conductivity of the two polymers is the same. Thus it appears that the position of the cyano group in the polymer, which influences so strongly the optical parameters, is not influential toward the conduction properties, which may reflect a similar intersite hopping distance.

(40) Zotti, G.; Martina, S.; Wegner, G.; Schluter, A. D. *Adv. Mater.* **1992**, *4*, 798.

(41) Schlenoff, J. S.; Chien, J. C. W. *J. Electrochem. Soc.* **1987**, *134*, 2179.

(42) Bredas, J. L.; Themans, B.; Fripiat, J. G.; Andre, J. M.; Chance, R. R. *Phys. Rev. B* **1984**, *29*, 6761.

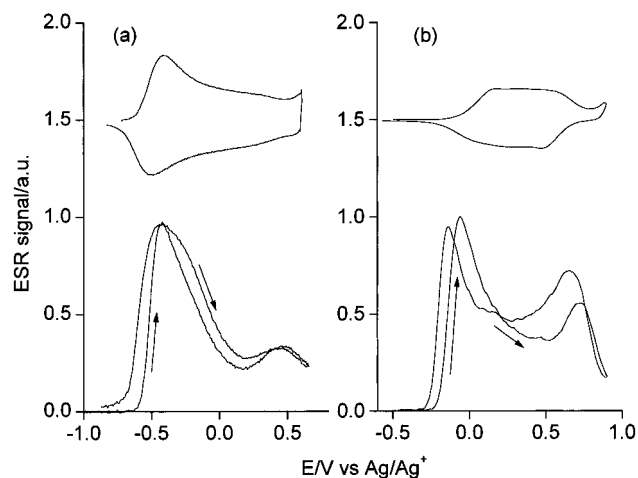


Figure 10. In situ ESR vs potential of (a) poly(1) and (b) poly(9) in AN + 0.1 M Bu₄NClO₄. Cyclic voltammograms for comparison.

A conductive behavior completely different from that of SYM polymers is displayed by ASYM polymers, in the sense that they do not show a limited potential window of conductivity. The shape of the conductivity–potential relationship in poly(6) is sigmoidal, with only a slight decrease with potential after the maximum (Figure 8c), despite the expected strong localization of the charge. A strictly similar behavior is shown by poly(7) and poly(8). It is conceivable that the asymmetry of the monomers causes a random sequence of linkages (head–head, head–tail, and tail–tail) between the monomeric units in the polymer. Therefore the absence of localization of conductivity might be attributed in these cases to disorder. The conductivity of poly(6) is relatively high (2 S cm⁻¹) due to the fact that linear cyano substituents at the ethylene moiety do not produce twisting of the polyconjugated chain.

In Situ ESR of the Polymers. In situ ESR of poly(1) during oxidation shows the appearance of a signal which reaches its maximum at a potential corresponding to E_1^o (Figure 10a) with a maximum spin concentration comparable with that measured in polypyrrole.⁴³

At higher potentials the signal decreases, then increases again with a significant relative maximum of spin concentration in proximity of E_2^o and finally disappears. This twin feature of the ESR signal vs potential relationship is common to all SYM polymers, being mostly evident in poly(9) (Figure 10b), whereas in the ASYM polymers only the first ESR maximum is observed. The presence of ESR maxima in correspondence of the redox peaks limiting the CV window is a feature already encountered in the case of polyaniline.⁴⁴ Partial occupancy of the band by holes and electrons at the upper and lower band edges respectively results in the appearance of unpaired electrons. Therefore ESR has given further support to the occurrence of band narrowing in SYM polymers and has provided a tool for the definition of band edges in cases in which CV peaks are not clearly displayed.

Bandwidth and Conductivity Windows. As for conducting materials in general, the conductivity of polyconjugated polymers is associated with the presence

of partially filled bands so that conduction is limited in the potential range by the depletion of the valence band. This was experimentally shown for many polymers including the main members polyaniline, polythiophene, and polypyrrole.⁴⁵

The bandwidth (BW), i.e., the width of the upper occupied π -band, of the nondoped polymer is obtained experimentally by UPS^{46,47} or XPS,⁴⁸ but it may be measured also by CV. In this case the voltammogram is a representation of the density-of-state function of the material,⁴⁹ and the bandwidth is given by the potential range of the CV process $\Delta E^o (=E_2^o - E_1^o)$. For a comparison of the methods, the calculated BW in, e.g., polythiophene (2.6–2.9 eV^{50–52}) is in reasonable agreement with the experimental value of ca. 3.2 eV by UPS⁴⁷ and ca. 2.5 eV by CV. The latter value was in fact obtained for the alkoxy-substituted polythiophene poly(4,4'-dimethoxydithiophene),⁵³ but substitution may to a first approximation be assumed to change significantly only the Fermi level.⁵⁴ It must be mentioned that the CV-measured BW may be changed as the counteranion is changed since charge pinning by nucleophilic anions make the oxidation of polypyrrole shift to lower potentials.^{55,56} This drawback may be in any case overcome by the use of noncoordinating anions such as perchlorate, which we have done in the present investigation. Finally the voltammetric BW may be narrower than expected from calculations on the neutral state because of band evolution during the doping process,⁴² but this requires extensive chemical changes comparable to those occurring in polyaniline during the leuco-emeraldine–pernigraniline transition.^{44,57}

If we consider the conductivity width CW in relation with the bandwidth BW we may observe that CW (measured at 50% of maximum conductivity) and ΔE^o are almost the same. In the case of polyaniline CW = ca. 0.5 V⁴⁵ vs $\Delta E^o = 0.6$ V; for poly(3,4-dimethylpyrrole) CW = 1.0 eV and $\Delta E^o = 1.3$ V,⁴⁵ while for polyacetylene CW = 1.2 eV and $\Delta E^o =$ ca. 1.5 V.⁵⁸ From Table 2 this appears to hold also for the polymers presently investigated. Therefore we may assume that BW and CW are intimately related and conclude that a modulation of CW will follow a corresponding variation of BW.

Conductivity Windows in A–D Polymers. Continuing the previous reasoning, a decrease of the polymer CW may be accomplished by reducing the BW, which in its turn may be achieved by an increase of the

(45) Ofer, D.; Crooks, R. M.; Wrighton, M. S. *J. Am. Chem. Soc.* **1990**, *112*, 7869.

(46) Distefano, G.; Jones, D.; Guerra, M.; Favaretto, L.; Modelli, A.; Mengoli, G. *J. Phys. Chem.* **1991**, *95*, 9746 and references therein.

(47) Jones, D.; Guerra, M.; Favaretto, L.; Modelli, A.; Fabrizio, M.; Distefano, G. *J. Phys. Chem.* **1990**, *94*, 5761.

(48) Wu, C. R.; Nilsson, J. O.; Inganäs, O.; Salaneck, W. R.; Osterholm, J. E.; Bredas, J. L. *Synth. Met.* **1987**, *21*, 197.

(49) Focke, W. W.; Wnek, G. E. *J. Electroanal. Chem.* **1988**, *256*, 343.

(50) Burke, L. S.; Cao, J.; Lilly, A. C. *J. Comput. Chem.* **1987**, *8*, 107.

(51) Bakhshi, A. K.; Ladik, J.; Seel, M. *Phys. Rev. B* **1987**, *35*, 704.

(52) Bredas, J. L.; Elsenbaumer, R. L.; Chance, R. R.; Silbey, R. J. *Chem. Phys.* **1983**, *78*, 5656.

(53) Dietrich, M.; Heinze, J. *Synth. Met.* **1991**, *41–43*, 503.

(54) Bredas, J. L.; Heeger, A. J.; Wudl, F. *J. Chem. Phys.* **1986**, *85*, 4673.

(55) Zotti, G.; Schiavon, G.; Comisso, N. *Synth. Met.* **1991**, *40*, 309.

(56) Li, Y.; Quian, R. *Synth. Met.* **1988**, *26*, 139.

(57) Glarum, S. H.; Marshall, J. H. *J. Phys. Chem.* **1988**, *92*, 4210.

(58) Park, L. Y.; Ofer, D.; Gardner, T. J.; Schrock, R. R.; Wrighton, M. S. *Chem. Mater.* **1992**, *4*, 1388.

(43) Zotti, G.; Schiavon, G. *Chem. Mater.* **1991**, *3*, 62.

(44) Glarum, S. H.; Marshall, J. H. *J. Electrochem. Soc.* **1987**, *134*, 2160.

inter-ring torsion angle. This has been shown theoretically in the case of polythiophene, polypyrrole, and polyparaphenylene⁵⁹ and in practice has been achieved with poly(3,4-cyclopentane-pyrrole), in which case the theoretical 3.8 eV value of the BW of polypyrrole⁶⁰ has been lowered to ca. 1.3 eV.⁶¹

Another approach, which we have applied in this work, is the alternation of electron-rich and electron-deficient moieties. Band narrowing has been shown to occur in regular copolymers.^{62–64} In the context of this work we have calculated the electronic properties (including BW) of two basic structures in SYM polymers, poly(1) and poly(4), and we have compared those results with the data obtained previously from the corresponding homopolymers polypyrrole, polyacetylene, and polythiophene. The theoretical calculations consisted first in the geometry optimization of the polymer chain using the Austin Model One (AM1) semiempirical Hartree–Fock method,⁶⁵ then on the evaluation of the polymer electronic structure with the nonempirical valence effective Hamiltonian (VEH) technique.⁶⁶

We indeed find valence band narrowing in poly(1) and poly(4) compared to the homopolymers. The calculated BW values are 1.75 and 1.0 eV for poly(1) and poly(4), respectively, i.e., definitely lower than BW of polypyrrole (3.8 eV⁶⁰), polyacetylene (6.5 eV⁶⁷), and polythiophene (2.6 eV⁵²). Since the evolution of conductivity is related to the depletion of the valence band, this theoretical result appears to be qualitatively consistent with the experimental data of Table 2 and Figures 7 and 8. Within the potential range considered in the experiments the valence band of polypyrrole, which is quite broad, is not likely to be fully depleted and the conductivity is not suppressed. In contrast, since the BW of poly(1) and poly(4) are much narrower, their valence band may well be depleted in the same potential range, which would explain the loss of conductivity. It is also noteworthy that the smaller BW of poly(4) relative to poly(1) (1.0 vs 1.75 eV) is consistent with the decrease of CW observed experimentally (Table 2). The fact that the voltammetric BWs are narrower than those calculated may be explained by the occurrence of some extent

of band evolution during the doping process. Finally the calculated electronic structures of periodic and nonperiodic copolymers of thiophene and isothianaphene⁶⁴ have confirmed that the absence of potential-localized conductivity observed in ASYM polymers corresponds to a smearing of the valence subbands of the corresponding SYM polymers into a single featureless band.

To better and more generally understand the valence band narrowing caused by A–D alternation in regular copolymers, we may take into consideration the difference between the valence band energies of the homopolymers (given as E°_{ox} in Table 3 and shown in Figure 4) since the higher their difference the stronger the charge localization at the more oxidizable site in the oxidized polymer. In practice we observe that the 0.1 eV difference between the valence band levels of the homopolymers relevant to poly(1,2-dithienylethylene) and poly(3) does not give a significant charge localization but the corresponding difference of 0.7 V for poly(4) or 1.65 V for poly(5) does yield significant localization. A comparison of the widths in Table 2 makes clear that the narrowing is increased from the ethylene to the thiophene bridge, i.e., from a singly to a doubly conjugated ethylene group, whereas longer conjugated sequences, such as the four conjugated ethylene groups in poly(9) and poly(10) do not reduce the width further.

From still another point of view, our polymers may be considered as structures intermediate between polypyrrole, which is oxidized starting from $E^{\circ} = -0.6$ V in a long CV plateau, theoretically 3.8 eV wide,⁶⁰ and a polymer containing isolated dipyrrole units which would undergo a one-electron oxidation at $E^{\circ} = 0.23$ V⁴⁰ in a narrow (0.09 V wide) redox bell-shaped process.³⁸ Thus in our cases the values of the redox potentials fall in the intermediate potential range (with the only exception of the cyano-activated poly(10)) and ΔE° 's (and therefore also CWs) are comprised between 0.7 and 0.35 V. The conjugative bridges make CW higher the stronger the interaction between the dipyrroles, which explains the wider CV response for poly(1). Increasing the length of the bridges does not significantly decrease the interaction nor, consequently, the CW.

Finally it is interesting to mention that the literature reports another case of limited potential window of conductivity comparable to ours and right in the case of an A–D alternating SYM polymer. Poly(2,5-dialkoxy-*p*-phenylenethynylene), in which dialkoxyphenylene (D) and ethynylene (A) groups alternate, does give rise to a finite window of conductivity without complete depletion of the band.⁶⁸

Conclusions

Regular copolymers of pyrrole and variously substituted ethylene, arylene, or heteroarylene units have been produced as thin films by anodic coupling of dipyrrolyl–ethylenes, –arylenes, or –heteroarylenes in acetonitrile. The resulting alternation of electron-acceptor and -donor moieties in these polyconjugated polymers reduces dramatically the width of the valence band, evidenced by potential-limited redox processes in cyclic voltammetry. Accordingly, potential windows of conductivity are displayed with a limited width in the range 0.35–0.7 V. The behavior of these A–D alternating polymers, which is intermediate between that of polypyrrole (with a valence band 3.8 eV wide) and that

(59) Bredas, J. L.; Street, G. B.; Themans, B.; Andre', J. M. *J. Chem. Phys.* **1985**, *83*, 1323.

(60) Bredas, J. L.; Themans, B.; Andre', J. M. *J. Chem. Phys.* **1983**, *78*, 6137.

(61) Goedel, W. A.; Holz, G.; Wegner, G.; Rosenmund, J.; Zotti, G. *Polymer* **1993**, *34*, 4341.

(62) Hong, S. Y.; Marynick, D. S. *Macromolecules* **1992**, *25*, 3591.

(63) Montheard, J. P.; Boiteux, G.; Themans, B.; Bredas, J. L.; Pascal, T.; Froyer, G. *Synth. Met.* **1990**, *36*, 195.

(64) Bakhshi, A. K.; Liegener, C. M.; Ladik, J. *Synth. Met.* **1989**, *30*, 79.

(65) Dewar, M. J. S.; Zoebisch, E.; Healy, E.; Stewart, J. J. P. *J. Am. Chem. Soc.* **1985**, *107*, 3902.

(66) Andre', J. M.; Bredas, J. L.; Dehalle, J.; Vanderveken, D. J.; Fripiat, J. G. In *Modern Techniques in Computational Chemistry*; Clementi, E., Ed.; ESCOM: Leiden, 1990, p 745.

(67) Bredas, J. L.; Chance, R. R.; Silbey, R.; Nicolas, G.; Durand, P. *J. Chem. Phys.* **1981**, *75*, 255.

(68) Ofer, D.; Swager, T. M.; Wrighton, M. S. *Chem. Mater.* **1995**, *7*, 418.

(69) Chung, T. C.; MacDiarmid, A. G.; Feldblum, A.; Heeger, A. J. *J. Polym. Sci. Polym. Lett.* **1982**, *20*, 427.

(70) Fouletier, M.; Armand, M.; Audier, M. *Mol. Cryst. Liq. Cryst.* **1985**, *121*, 333.

(71) Hankin, A. G.; North, A. M. *Trans. Faraday Soc.* **1967**, *63*, 1525.

(72) Bauerle, P. *Adv. Mater.* **1992**, *4*, 102.

(73) Rhode, N.; Eh, M.; Geissler, U.; Hallensleben, M. L.; Voigt, B.; Voigt, M. *Adv. Mater.* **1995**, *7*, 401.

(74) Schiavon, G.; Zotti, G.; Bontempelli, G. *J. Electroanal. Chem.* **1984**, *161*, 323.

of a polymer bearing noninteracting dipyrrole units (with a valence band 0.09 eV wide), is explained by charge localization on the electron-rich dipyrrole segments in the polymer. The exceptional stability toward overoxidation of the polymer obtained from dipyrrolythiophene has evidenced the sequential display of two potential windows of conductivity along the potential scale.

The discovery of multiple and electrochemically modulated potential windows of conductivity in polyconjugated polymers might be useful for the development of new organic electronic devices.

Acknowledgment. J. L. Bredas and A. Pohl (Université de Mons-Hainaut) are gratefully acknowledged

for helpful discussions. Work on conjugated polymers in Mons is partly supported by Belgian Government in the framework of "Pole d'Attraction Interuniversitaire en Chimie Supramoléculaire et Catalyse", FMRS-FRFC and an IBM Academic Joint Study. This work is supported by the European Commission Human Capital and Mobility network on "Functional Materials Organized at Supramolecular Level" and "Synthetic Electroactive Materials". R.L. is chercheur qualifié du Fonds National de la Recherche Scientifique. The authors would like to thank R.Salmaso and S.Sitran of the CNR for their technical assistance.

CM9702140